Available online at www.sciencedirect.com
SCIENCE DIRECT®
Journal of Nuclear Materials 337–339 (2005) 1082–1086
journal of nuclear materials
www.elsevier.com/locate/jnucmat

Rovibrational distribution of H_2 in low temperature plasma: the dependence on the plasma parameters

Bingjia Xiao [a,b,*], Shinichiro Kado [b], Shin Kajita [c], Daisuke Yamasaki [c], Satoru Tanaka [c]

[a] Institute of Plasma Physics, Chinese Academy of Sciences, P.O. Box 1126, Hefei Anhui 230031, P.R. China
[b] High Temperature Plasma Center, The University of Tokyo, Yayoi 2-11-16, Bunkyo-Ku, Tokyo 113-8656, Japan
[c] Department of Quantum Engineering and Systems Sciences, The University of Tokyo, Hongo 7-3-1, Bunkyo-Ku, Tokyo, Japan

Abstract

Fulcher-α band emissions were fitted using the Boltzmann distribution for the rotational and vibrational distribution of hydrogen molecules in MAP-II plasmas. The dependency of the rovibrational temperatures on the neutral pressure are explored in the cases of the helium discharges with H_2 puff and pure H_2 discharges. It was found that the rotational and vibrational temperatures increase with the electron temperatures in the experimental conditions studied. However, the opposite trend is predicted by our modeling, in which the newest cross section data are applied in the most important kinetic processes included in vibrational population balance based on the quasi-steady state and quasi-stationary approximation. The possible channels to cause the discrepancy are discussed; however, the physical mechanism behind remains un-discovered.

PACS: 33.20.Kf; 33.20.Vq; 34.80.Gs
Keywords: Hydrogen; Spectroscopy; Neutral modeling; Divertor diagnostics; MAP-II

1. Introduction

Vibrational excitation is one of the key factors for the negative ion production [1,2] and for the hydrogen molecular behaviors in the edge plasmas [3]. This paper focuses on the dependency of H_2 vibrational distribution on the plasma parameters, especially on the electron temperature and the neutral pressure. In Section 2, we discuss the modeling of H_2 vibrational distribution and the processes therein. In Section 3, we give a brief introduction of the experimental determination of the distribution from Fulcher-α band spectroscopy and the experimental setup. Based on the comparisons of the experimental and modeling results, finally we give our discussions and hence the summary.

2. Modeling of H_2 vibrational distributions in low temperature plasmas

In low temperature plasmas, hydrogen molecules can be vibrationally excited in mainly two ways. In

* Corresponding author. Tel.: +86 551 5591 397; fax: +86 551 5591 310.
E-mail addresses: bjxiao@ipp.ac.cn (B. Xiao), kado@q.t.u-tokyo.ac.jp (S. Kado).

0022-3115/$ - see front matter © 2004 Elsevier B.V. All rights reserved.
doi:10.1016/j.jnucmat.2004.10.025

low electron energy range of the order of several electron Volt, the incident electrons can attach to the target hydrogen molecules to form negative H_2^- molecules which are mainly in the resonant electronic states of $^2\Sigma_g^+$ and $^2\Sigma_g^+$. These H_2^- molecules can either be dissociated or detach the attached electrons to return to H_2. The latter process causes the enhanced vibrational excitation as shown by Bardsley's theoretical results using a resonant theory [4]. When the electron energy is higher to above ~14 eV, H_2 can be excited to the higher electronic states, i.e., $B^1\Sigma_u^-$ and $C^1\Pi_u$ states. These excitations will be followed by simultaneous photon emission to return to the ground electronic state. This also causes the molecules in ground electronic state to be distributed in higher vibrational states. After the molecules gain the vibrational quanta, they would redistribute via the vibrational exchange among H_2, or vibrational de-excitation through vibration–translational exchange via the collisions with both the neutrals and the charged ions. In addition, H_2 can also be dissociated or be ionized. Because the ionization and dissociation processes have the dependency on the vibrational level of the molecules, they also play important roles in the vibrational distribution. Generally, H_2 at higher vibrational levels have higher possibilities to be dissociated or to be ionized, so the dissociation or the ionization mostly causes vibrational de-excitation. To determine the vibrational distribution, one can rely on the so-called quasi-steady and quasi-stable model for the equilibrium of the hydrogen molecules in different vibrational states which has been discussed in detail by Gorse [1], Kreshinnikov [3] and Pigarov [5] etc.,

$$\sum_i \left(\frac{dN_v}{dt}\right)_i = 0. \tag{1}$$

The summation must be performed on all possible processes which are effective in the system in the contributions to the generation and depletion of the molecules in vibrational states v which ranges from 1 to 14. If the molecules in primarily vibrationally ground state can be determined by the transport or the other methods and the time to reach vibrational equilibrium is much shorter in comparison to the transport time of the molecules, then the populations of the molecules in vibrationally excited states can be solved against the population of the molecules in vibrational ground state.

Table 1 summarized all the processes which are considered in this paper. Most of the complete sets of vibrationally resolved electron impact cross sections can be found in Celiberto's compilation [6] except those for the excitation to the triplet states and the e–v process. For the excitation to the triplet states, we use Gryzinski's method [12,13] to obtain the complete sets of the vibrational resolved cross sections.

Table 1
Kinetic process of H_2 in low temperature plasmas

e–v	$e + H_2(v) \rightarrow H_2^- \rightarrow e + H_2(w)$	[4]
e–DA	$e + H_2(v) \rightarrow H_2^- \rightarrow H + H^-$	[4,5]
e–D	$e + H_2(v) \rightarrow H_2(b^3\Sigma_u^-) \rightarrow H + H$	[6]
e–D	$e + H_2(v) \rightarrow H_2(a^3\Sigma_u^+, c^3\Pi_u, e^3\Sigma_u^+, d^3\Pi_u)$	This work
E–V	$H_2(v) + e \rightarrow H_2(B^1\Sigma_u^-, C^1\Pi_u) + e \rightarrow H_2(w) + e$	[6]
Ionc	$H_2(v) + H^+ \rightarrow H_2^+ + H$	[7,8]
p–v	$H_2(v_i) + H^+ \rightarrow H_2(v_f) + H^+$	[8,9]
e–DE	$H_2(v) + e \rightarrow H_2(\Sigma_u^-, C^1\Pi_u) + e \rightarrow H + H$	[6]
e–I	$H_2(v) + e \rightarrow H_2^+$	[6]
e–ID	$H_2(v) + e \rightarrow H + H^+$	[6]
v–v	$H_2(v) + H_2(w+1) \rightarrow H_2(v+1) + H_2(w)$	[10]
v–t	$H_2(v) + A \rightarrow H_2(w) + A$ $(v > w)$	[10,11]

For the e–v cross sections, we utilized the Bardsley's cross sections [4] for 0–w ($1 < w < 6$, 0 and w are the initial and final vibrational levels, respectively) transitions. Necessary electron energy extrapolation was made to get the reaction rate coefficients. For the transition v–w ($v > 0$, $w > v$), we utilize the scaling law suggested by C. Gorse [14],

$$\sigma_{1\rightarrow w} = w\sigma_{0\rightarrow w-1}(1 < w < 6)$$

$$\text{and } \sigma_{v\rightarrow w} = \sigma_{v-1\rightarrow w-1} = \cdots = \sigma_{1\rightarrow w-v+1}(w >= 2). \tag{2}$$

For the v change larger than 5, we just simply take the cross sections to be zero as they indeed are negligibly small.

For the process of vibrational exchange, according to [10], the forward v–v reaction rate coefficients in Table 1 can be approximated by:

$$R_{v,w} \approx (v+1)(w+1)R_{0,1}\left(\frac{3}{2} - \frac{1}{2}e^{-\delta(v-w)}\right) \times \exp\left[\Delta_1(v-w) - \Delta_2(v-w)^2\right] \quad v > w, \tag{3}$$

where $R_{0,1} \approx 4.23 \times 10^{-15}(300/T_g)^{1/3}$ $cm^3 s^{-1}$, $\delta \approx 0.21(T_g/300)^{1/2}$, $\Delta_1 \approx 0.236(T_g/300)^{1/4}$, $\Delta_2 \approx 0.0572(300/T_g)^{1/3}$ and T_g is the gas temperature in Kelvin. The reverse reaction is also possible but the reaction rate is less than the forward one by an exponent factor,

$$R'_{v,w} = R_{v,w}\exp\left[G(v+1) + G(w) - G(v) - G(w+1)\right]/T_e, \tag{4}$$

where G denotes the vibrational energy. The v–t relaxation occurred among the molecules and hydrogen atoms can be found in Gorse [14]. For the vibrational translational exchange, we only consider hydrogen molecules and atoms because they are the main heavy species in most of the divertor plasmas. For the v–t exchange with hydrogen molecules, we use the following formula which

was derived by Matveyev [10] based on the results of Caccitore [11],

$$R_{v,v-1}^{H_2(w),vt} = 7.47 \times 10^{-12}\sqrt{T_g}\exp(-93.87T_g^{-1/3})v \times \exp\left[\delta_{VT}(v-1) + \delta'_{VT}w\right] \text{ cm}^3/\text{s}, \quad (5)$$

where $\delta_{VT} \approx .97(300/T_g)^{1/3}$ and $\delta'_{VT} \approx .287(300/T_g)^{1/2}$.

For the proton impact processes, mainly ion conversions and proton induced vibrational excitations, Janev [8] summarized the current database and gave the relevant scaling laws. In MAP-II plasma, H_2 density is about 2 orders higher than electron density. In this case, H_2^+ and H^+ may have considerable fractions so that H^+ is not the only important ion species and its density is lower than the electron density. Moreover, because there is no enough time for the ion-electron collisions, ion temperature is generally lower than the electron temperatures. Exact determination of these quantities is not applicable so the exact consideration of these processes is not currently possible. Fortunately as one could see from the discussion section of this paper, neither the p–v nor the ion conversion processes play important roles in the explanation of our experimental observation. In the modeling, we simply assume that the ion temperature and density are the same with electrons.

3. Experimental determination of H_2 rovibrational distribution

In many researches such as Fantz [15], Surrey [16] and our previous work [17] etc., Fulcher-α band spectroscopy was used for the diagnostics of the H_2 vibrational distribution in low temperature plasmas. In these studies, the vibrational distribution of H_2 in the electronic ground state was taken to be Boltzmann distribution characterized by the vibrational temperature. In our previous work, we further found that the rotational distribution in the electronic ground state particularly obeys the Boltzmann distribution. Thus in this paper to fit the experimental observed emissions we use also the following function, which was explained in detail in our previous publication [17],

$$I_{av''J''}^{dv'J'} = \frac{hc}{\lambda}\frac{A_{av''J''}^{dv'J'}}{A_{tot}} \times \sum_v \sum_J \left\{ R_{XvJ}^{dv'J'} C_v (2J+1) g_{as} \times \exp\left[-\frac{F_X(J,v)}{T_{rot}} - \frac{G_X(v)}{T_v}\right]\right\}. \quad (6)$$

$I_{av''J''}^{dv'J'}$ and $A_{av''J''}^{dv'J'}$ are the emission intensity and the radiative emission rate coefficient, respectively. v denotes the vibrational level and J rotational level. R is the rovibrationally resolved electron impact reaction rate, $n_e\langle\sigma v\rangle$. F is the rotational energy and G the vibrational energy. g_{as} is the degeneracy factor to consider the nuclear spin and C_v is a normalization factor. The summation in the formula are performed on all possible v and J values.

The experiment was done in MAP-II device (Material and Plasma) which was designed to be an edge plasma simulator. The details of the device and the experimental setup has been provided in former publications [17,18]. After an arc discharge between a flat LaB_6 cathode and an anode pipe, the plasma is confined by a longitudinal magnetic field of ~200 Gauss to form a column with a diameter of ~5 cm. It is transmitted to the target chamber and finally stopped at a floating target. Secondary gas can be injected into the target chamber. Langmuir probes are used to measure the electron temperature and density. In the target chamber, the electron temperature can be varied from lower than 1 eV to about 10 eV, and the electron density can be varied from 10^{11} to 10^{12} cm^{-3} by adjusting the discharge voltage and current and the gas pressure.

For the optical spectroscopy, a 1 m Czerny-Turner monochromator with a 1200 grooves/mm grating equipped with a photo-multiplier tube was used. The wavelength resolution was about 0.042 nm at a 50 μm slit width. Line emission was collected by the spectrometer across the column so that the collected signals are indeed the radial line integral. The line integration effect can be taken into consideration using the same way which we did in our previous work [17].

4. Results and discussion

Fig. 1 gives the solution results of the Eq. (1). The ratio of the H_2 density with respect to the electron density was set to be 100 which is close to the experimental conditions. It can be seen that when the vibrational level is less than 5, the absolute curve slope of the distribution decreases with the decrease of the electron temperature. This implies that the vibrational temperature is predicted to be a decreasing function as to the electron

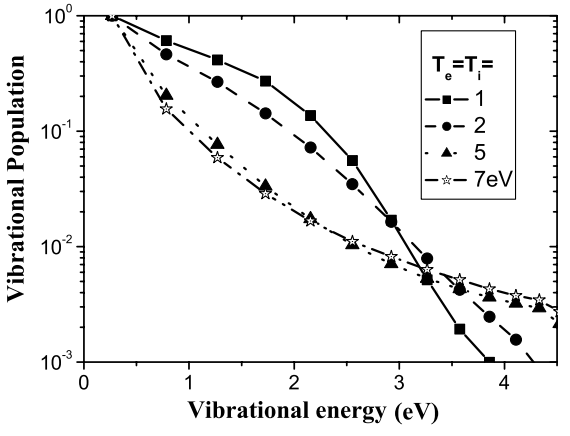

Fig. 1. Modeling result: vibrational distribution as a function of electron temperature.

temperature if we approximate the vibrational distribution in lower vibrational level to be Boltzmann. However, both the measured vibrational and rotational temperatures decrease as functions of the neutral pressure in both the helium discharge with H_2 puff and pure H_2 discharge as shown in Fig. 2. When the neutral pressure goes higher, the electron temperature would decrease because more energy is transferred from the electrons to the neutrals. It also brings about more cooling to the rotationally excited H_2 so that the rotational temperature goes down. As to the vibrational temperature dependency on the electron temperatures, the experiment shows the opposite trends compared with that predicted by the modeling. We noticed that in Fantz' experiment [19], the same dependency of the vibrational temperature on the neutral pressure existed when the D_2 pressure is less than 5 Pa. However, the dependency became reversed as the D_2 pressure is larger than 5 Pa. Unfortunately we have no information in Fantz's reported results for the electron temperature.

We discuss the possible channels which might cause the discrepancy between our experiment and our theoretical prediction on the vibrational temperature dependence on the neutral pressure or electron temperature. From the view point of the experiment, one may think that it is possibly due to our assumed vibrational distribution. The vibrational distribution may not obey well the Boltzmann, which we adopted in our experimental data analysis. However, the fitting in all the cases shows less than 10% uncertainties for the vibrational temperature. This implies that the vibrational temperature at least reflects the initial slope of the vibrational distribution curve. The experiment also depends on the applied vibrationally resolved reaction rate for the excitation from the ground state to the upper Fulcher state. Detail discussion about the cross sections and the reaction rates can be found in again our previous work [17]. As a try, we used the Fantz's treatment [15] for the reaction rates, the derived vibrational temperature exceeds our values by percentages about ~10%. This did not change our experimental finding that the vibrational temperature to be a decreasing function as to the electron temperature.

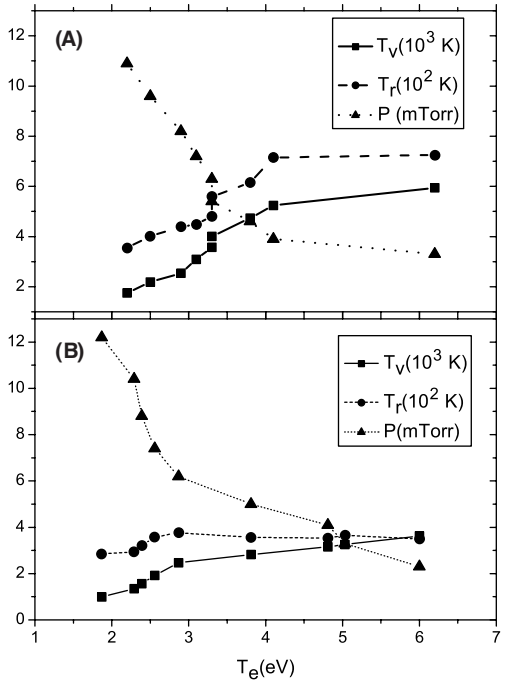

Fig. 2. Measured rotational and vibrational temperatures. (A) Helium discharge using H_2 puff, (B) H_2 discharge using H_2 puff.

The vibrational exchange might also be one of the causes. Generally, vibrational exchange would make the final equilibrium distribution to be,

$$N(v) = N_0 \exp\left(-\frac{\varpi v}{kT_v} + \frac{\varpi_x v(v+1)}{kT}\right), \tag{7}$$

where $\varpi$and ϖ_x is the molecule term values and T is the temperature of the molecules which can be approximately taken to be the rotational temperature in most of the cases. This equilibrium can only occur or be assumed when the v–v exchange collision frequency is much larger than the other processes. For ($v = 3$, $w = 2$) → ($v = 4$, $w = 1$), the v–v rate coefficient is only 1.41×10^{-14} cm^3/s. For the smaller initial v and w, the value is even smaller. This is negligibly small in comparison with e–v rate coefficients at electron temperature of 3 eV, which is 1.9×10^{-9} cm^3/s for $0 \rightarrow 1$ transition. So in lower vibrational levels, v–v exchange can be neglected if the molecules density is less 4 orders higher than the electron density.

At low electron temperatures ($T_e \sim 3$ eV), the dominant collision to determine the vibrational distribution is the electron attachment process. For example at $T_e = 3$ eV, for the process H_2 ($v_i = 0$) + e → e + H_2^- → e + H_2 ($v_f = 1$), the rate coefficients is about 1.9×10^{-9} cm^3/s. The p–v process may compete with the e–v processes. When the ion temperature is close to the electron temperatures (1–7 eV), the 0–1 p–v excitation rate coefficient is in the range of $0.2–0.5 \times 10^{-9}$ cm^3/s which is much smaller than the e–v reaction rates. The other contributions are at least several times lower than e–v process. Concerning the depletion rates of the state $v = 1$, the total reaction rate coefficients for the electron attachment including dissociation attachment is 6.2×10^{-9} cm^3/s. This is the most dominant depletion process for the state $v = 1$, in comparison with the other depletion processes. The vibrational population at $v = 1$, is thus determined by the balance between these two processes. Namely, $N(v = 1) \sim N(v = 0) R_{e-v}$ ($v = 0–1$)/R_{attach} ($v = 1$). Our underlying database for this process is all originated from Bardsley's calculation [4]. Necessary extrapolation

was made to the electron energy beyond the range of $2\,eV < E_e < 12\,eV$. The extrapolation should not influence much the exactness of the rate coefficients at electron temperature of 3–6 eV which is of our interest.

It may not exactly reflect the cross sections calculated by Bardsley [4] for the scaling by Gorse [14] which was used in this paper. However, the $0(v_i) - 1(v_f)$ cross section is slightly more than one half of the $1(v_i) - 2(v_f)$ cross section when we check Bardsley [4] cross section at 6 and 8 eV. This small difference should not change much the relative slope of the vibrational distribution. This point was verified by [20] when using a different scaling law which was suggested by Pigarov [5].

5. Summary

In summary, we have observed that the vibrational temperature is a decreasing function as to the neutral pressures and thus to the electron temperature in the case of the discharge characterized by the neutral pressure of 2–16 mTorr and the electron temperature of 1–6 eV. This dependency is just the opposite of that predicated by our modeling. Our current knowledge cannot explain the physical mechanism behind. There are possibilities of the $H_2 - H_2^+$ and $H_2 - H_3^+$ collisions which contribute to the observed vibrational distribution, however, current understanding by either us or the literature is limited. To discover the physical mechanism behind the observed distribution is our future objective.

Acknowledgments

One of the authors, B. Xiao acknowledges the partial support by NSFC with grants No. 10135020 and 10275067. This work was done during his stay in Univ. Tokyo as a guest researcher.

References

[1] C. Gorse, R. Celiberto, et al., Chem. Phys. 161 (1992) 211.
[2] J.R. Hiskes, A.M. Karo, Appl. Phys. Lett. 54 (6) (1989) 508.
[3] S.I. Krasheninnikov et al., Phys. Lett. A 214 (1996) 285.
[4] J.N. Bardsley, J.M. Wadehra, Phys. Rev. A 20 (1979) 1398.
[5] A.Yu. Pigarov, Phys. Scr. T96 (2002) 16.
[6] R. Celeiberto, R.K. Janev, A. Larricciuta, M. Capitelli, J.M. Wadehra, et al., Atomic Data.
[7] A. Ichihara, O. Iwamoto, R.K. Yanev, J. Phys. B: At. Mol. Opt. Phy. 33 (2000) 4747.
[8] R.K. Janev, D. Reiter, U. Samm, FZJ report, 2003.
[9] http://www-cfadc.phy.ornl.gov/h2mol/molh2.html.
[10] A. Matveyev, V.P. Silakov, Plasma Sources Sci. Technol. 4 (1995) 606;
Nuclear Data Tables 77 (2001) 161.
[11] M. Cacciatore, M. Capitelli, G.D. Billing, Chem. Phys. Lett. 157 (1989) 305.
[12] M. Gryzinski, Phys. Rev. 138 (2A) (1965) A305–A359.
[13] E. Bauer, C.D. Bartky, J. Chem. Phys. 43 (1965) 2466.
[14] C. Gorse, M. Capitelli, M. Bacal, J. Bretagne, A. Lagana, Chem. Phys. 117 (1987) 177.
[15] U. Fantz, B. Heger, Plasma Phys. Control. Fusion 40 (1998) 2023.
[16] E. Surrey, B. Crowley, Plasma Phys. Control. Fusion 45 (2003) 1209.
[17] B. Xiao, S. Kado, et al., Plasma Phys. Control. Fusion 46 (2004) 653.
[18] S. Kajita, S. Kado, N. Uchida, T. Shikama, S. Tanaka, J. Nucl. Mater. 313–316 (2003) 748.
[19] U. Fantz, Contri. Plasma Phys. 42 (2002) 675.
[20] M. He, Thesis, Institute of Plasma Physics, Chinese Academy of Sciences, 2004.